Eur. Phys. J. D (2016) 70: 249
DOI: 10.1140/epjd/e2016-70161-2

THE EUROPEAN PHYSICAL JOURNAL D

Regular Article

Signatures of laser photon energy in (e, 2e) reactions in helium

Abdelkader Makhoute[1], Imane Ajana[1,a], Driss Khalil[1], Abdelmalek Taoutioui[1,2], and Alain Dubois[2]

[1] Physique du Rayonnement et des Interactions Laser-Matière, Faculté des Sciences, Université Moulay Ismail, B.P. 11201, Zitoune, Meknès, Morocco
[2] Sorbonne Universités, UPMC University Paris 06, CNRS, Laboratoire de Chimie Physique-Matière et Rayonnement, 75231 Paris Cedex 05, France

Received 4 March 2016 / Received in final form 7 july 2016
Published online 22 November 2016 –

Abstract. Electron-impact ionization of helium target in the presence of a linearly polarized laser field is investigated at low incoming energy in the second Born approximation and in the asymmetric coplanar geometry. The status of incident and scattered electrons in the external laser field is described by the non-relativistic Volkov waves. The dressed state of the ejected electron is treated as a Coulomb-Volkov wave function. The laser polarization vector is taken to be parallel to the incident momentum of the projectile. The scattering amplitudes are performed by using the Sturmian basis. Numerical results show that the laser photon energy dependence of the angular distributions of the ejected electrons has a significant control on the (e, 2e) reactions. The structure of the triple differential cross section in the vicinity of resonances have been discussed. The higher order terms of the Born series of the scattering amplitude will be negligible compared to the first terms at high laser frequencies.

1 Introduction

The study of laser-assisted collisions between atoms and charged particles has attracted a great deal of attention in the recent years both from the theoretical and experimental perspectives [1–8]. In particular, the laser-assisted electron-atom ionization processes, called laser-assisted (e, 2e) reactions, play a very prominent role in many applied areas such as plasma heating, plasma confinement, high power gas lasers, gas breakdown. The availability of lasers in wide range of frequency, intensity and polarisation along with improved techniques of detection and resolution for laser and electrons allowed the realization of laser-assisted elastic and excitation scattering experiments on noble gazes [9–12]. Experiments in which laser-assisted collisions can be studied with full control over the kinematics and the laser beam parameters are difficult to realize. This is mainly due to the high laser intensities required and the necessity to overlap an incident electron beam with a tightly focused and pulsed laser beam in time and position. The first kinematically complete experiment of laser-assisted (e, 2e) collision was performed by Höhr et al. [13] for high incident electron energy of 1 keV. For a good comparison with experimental results of Höhr et al. [13], we need a relativistic treatment of the laser-electron interaction by using the relativistic volkov wave, and of the laser-target interaction by solving the Dirac equation.

One of the most delicate aspects of laser-assisted (e, 2e) reactions consists in providing an adequate description of the target states in the presence of the laser field. This problem is particularly acute when strong fields are considered, or when the laser frequency is nearly resonant with an atomic transition. Most theoretical studies of laser-assisted electron-atom collisions have been confined to the simple case in which the target atom is considered to be a structureless center of force, representing by a static potential [14–16]. Those studies have been useful in providing a detailed understanding of the role played by the laser-projectile interaction in the collisions processes. A laser-assisted (e, 2e) collisions treatment have been proposed [17], which is based on first-order time dependent perturbation theory in the laser-atom interaction, while the laser-projectile interaction is treated non perturbatively. It was found that the triply differential cross sections are strongly dependent on the "dressing" of the atomic target by the laser. At sufficiently high energies, it is generally believed that the first Born approximation (FBA) can be used to describe the direct ionization process [18]. It is therefore obviously necessary to extend the Born approximation by treating the projectile-target interaction up to second-order Born amplitude in the range of the low energy regime.

The laser parameters such as the intensity, the polarization, and in particular the laser photon energy has significant control on the (e, 2e) process. The influence of these parameters has attracted a great deal of attention in theoretical works [19–24]. In this paper, we want to show that the laser photon energy is a good control factor in the laser-assisted (e, 2e) collisions in helium at low energy regime by using the second Born approximation

[a] e-mail: ajanaimane@gmail.com

(SBA), in particular on the electron-electron interaction. The organization of the paper is as follows. In Section 2, we present the theory of laser-assisted (e, 2e) reactions in helium in the coplanar asymmetric geometry. Our second and first-order Born results are presented and discussed in Section 3. Section 4 summarizes on conclusions. Atomic units (a.u.) are used throughout this paper.

2 Theory

Let us consider the laser-assisted (e, 2e) reaction of helium target

$$e^-(E_{k_i}, \boldsymbol{k}_i) + \mathrm{He} + \ell\hbar\omega \longrightarrow \mathrm{He}^+ + e^-(E_{k_f}, \boldsymbol{k}_f) + e^-(E_{k_e}, \boldsymbol{k}_e), \quad (1)$$

where E_{k_i}, E_{k_f}, E_{k_e}, and $\boldsymbol{k}_i$, $\boldsymbol{k}_f$, $\boldsymbol{k}_e$ are the energies and the momentum of the incident, scattered and ejected electrons respectively. The positive integer values of ℓ correspond to photon absorption, negative integer values to photon emission and $\ell = 0$ to laser-assisted (e, 2e) reactions with no net transfer of photons.

The energy conservation equation corresponding to laser-assisted (e, 2e) reaction of equation (1) reads

$$E_{k_i} + E_0^{\mathrm{He}} + \ell\omega = E_0^{\mathrm{He}^+} + E_{k_f} + E_{k_e}. \quad (2)$$

In the last equation, E_0^{He} is the ground state energy of helium atom, while $E_0^{\mathrm{He}^+}$ represent the energy of the residual ion He^+.

We shall assume that the laser field is treated classically as a single mode, spatially homogenous, monochromatic, linearly polarized electric field with frequency ω and wave vector $\boldsymbol{k}$. A typical situation is when the laser wavelength $\lambda = \frac{2\pi}{\omega}$, where $\omega = kc$ and $c = 137$ a.u., is much greater than the spatial extent both of the target and the region where the electron-electron collision takes place. This validates the use of the dipole approximation for the electric component and vector potential of the laser field which are given respectively by

$$\boldsymbol{\mathcal{E}}(t) = \boldsymbol{\mathcal{E}}_0 \sin(\omega t), \quad \boldsymbol{A}(t) = \boldsymbol{A}_0 \cos(\omega t), \quad (3)$$

where $\boldsymbol{A}_0 = c\,\boldsymbol{\mathcal{E}}_0/\omega$. The electric field amplitude $\mathcal{E}_0$ and the laser frequency ω are supposed to be small on the atomic scale in order to discard possible photoionization effects.

To describe such a collision of two systems interacting with an external laser field, one can start by calculating the S-matrix element

$$S_{f,i} = -i \int_{-\infty}^{+\infty} dt \, \langle \Psi_f | \left(\hat{H} - i\frac{\partial}{\partial t} \right) | \Phi_i \rangle , \quad (4)$$

where Φ_i and Ψ_f are the initial and final states respectively of the colliding system embedded in the external electromagnetic background. $\hat{H}$ in equation (4) denotes the total Hamiltonian of the colliding system in the presence of the external laser field.

It is known that the S-matrix element is gauge-invariant. However, this properly can be violated if one uses approximation treatments, for example, such as time-dependant perturbation theory, when accounting for the laser field effect on electron states. In our model, we employ the length gauge, which gives more accurate perturbation results for laser-modified target states than the velocity gauge [25].

In the present model, the projectile-laser interaction is treated exactly to all orders and described in terms of a non relativistic Volkov wave function [26], which is solution of the Schrödinger equation for the electron motion in a plane electromagnetic wave. The interaction between the projectile and atomic target is treated within the SBA in the sense that the projectile interacts twice with the target. The main difficulty with the laser-assisted collisions consists in the description of the initial and final states of the target in the presence of the laser field. Since we are considering laser fields such that the electric field strength $\mathcal{E}_0$ is small with respect to the atomic unit of field strength $\mathcal{E}_0 = e/a_0^2 \simeq 5 \times 10^{11}$ V m^{-1}, we can use first-order time-dependant perturbation theory to obtain the explicit expression of the dressed ground-state wave function given in reference [27]. For the dressed continuum state of the ejected electron of asymptotic momentum $\boldsymbol{k}_e$ subjected to the combined influence of the laser field and the residual ion, we have used the wave function first proposed in references [20,21].

Once the S-matrix element of equation (4) is established, the ionization amplitude in the second Born approximation for the (e, 2e) process in the presence of a linearly polarized radiation field reads

$$f_{ion}^{\ell}(\boldsymbol{\Delta}) = f_{ion}^{B_1,\ell}(\boldsymbol{\Delta}) + f_{ion}^{B_2,\ell,0}(\boldsymbol{\Delta}), \quad (5)$$

where $f_{ion}^{B_2,\ell,0}(\boldsymbol{\Delta})$ is the second Born ionization amplitude of zeroth-order in $\mathcal{E}_0$ evaluated at the shifted momenta $\boldsymbol{\Delta}_i$ and $\boldsymbol{\Delta}_f$ with the transfer of ℓ photons [28,29]

$$f_{ion}^{B_2,\ell,0}(\boldsymbol{\Delta}) = -\frac{J_\ell(\lambda)}{\pi^2} \times \int_0^{+\infty} d\boldsymbol{q} \frac{\left\langle \psi_{k_e}^{(-)} \middle| \widetilde{V}_d(\boldsymbol{\Delta}_f, \boldsymbol{X}) G_c(\zeta) \widetilde{V}_d(\boldsymbol{\Delta}_i, \boldsymbol{X}) \middle| \psi_0 \right\rangle}{\Delta_i^2 \Delta_f^2}, \quad (6)$$

and $f_{ion}^{B_1,\ell}$ is the first Born amplitude for the laser-assisted (e, 2e) process involving the exchange of ℓ photons [20,21,28,29]

$$f_{ion}^{B_1,\ell}(\boldsymbol{\Delta}) = f_1(\boldsymbol{\Delta}) + f_2(\boldsymbol{\Delta}) + f_3(\boldsymbol{\Delta}), \quad (7)$$

with

$$f_1(\boldsymbol{\Delta}) = -2\Delta^{-2} \left\langle \psi_{k_e}^{(-)} \middle| \widetilde{V}_d(\boldsymbol{\Delta}, \boldsymbol{X}) \middle| \psi_0 \right\rangle J_\ell(\lambda), \quad (8a)$$

$$f_2(\boldsymbol{\Delta}) = i\Delta^{-2} \sum_j \left\langle \psi_{k_e}^{(-)} \middle| \widetilde{V}_d(\boldsymbol{\Delta}, \boldsymbol{X}) \middle| \psi_j \right\rangle M_{j0} \times \left(\frac{J_{\ell-1}(\lambda)}{E_j - E_0^{\mathrm{He}} - \omega} - \frac{J_{\ell+1}(\lambda)}{E_j - E_0^{\mathrm{He}} + \omega} \right), \quad (8b)$$

and

$$f_3(\boldsymbol{\Delta}) = i\Delta^{-2}\sum_j \left\langle \psi_j \middle| \widetilde{V}_d(\boldsymbol{\Delta},\boldsymbol{X}) \middle| \psi_0 \right\rangle M^*_{jk_e} \times \left(\frac{J_{\ell-1}(\lambda)}{E_j - E_{k_e} - E_0^{\mathrm{He}^+} + \omega} - \frac{J_{\ell+l}(\lambda)}{E_j - E_{k_e} - E_0^{\mathrm{He}^+} - \omega} \right) - 2\Delta^{-2}\boldsymbol{k}_e.\boldsymbol{\alpha}_0 J'_\ell(\lambda) \left\langle \psi^{(-)}_{k_e} \middle| \widetilde{V}_d(\boldsymbol{\Delta},\boldsymbol{X}) \middle| \psi_0 \right\rangle. \quad (8c)$$

In these equations, ψ_0 is the target ground-state wave function [20], the wave function $\psi^{(-)}_{k_e}$ describes the motion of the emitted electron in the continuum with momentum $\boldsymbol{k}_e$ in the presence of the Coulomb field of the residual ion [20,21] and ψ_j is a target state of energy E_j in the absence of the laser field [20,21]. $\boldsymbol{X}$ denotes the ensemble of target coordinates $r_1, r_2, \ldots, r_Z$. J_ℓ is a Bessel function of order ℓ, $\boldsymbol{\Delta} = \boldsymbol{k}_i - \boldsymbol{k}_f$ is the momentum transfer, $\boldsymbol{\Delta}_i = \boldsymbol{k}_i - \boldsymbol{q}$ and $\boldsymbol{\Delta}_f = \boldsymbol{q} - \boldsymbol{k}_f$ where $\boldsymbol{q}$ is the virtual projectile wave vector. $\lambda = \boldsymbol{\alpha}_0(\boldsymbol{\Delta} - \boldsymbol{k}_e)$ with $\boldsymbol{\alpha}_0 = \boldsymbol{\mathcal{E}}_0/\omega^2$ being the amplitude of oscillation of a classical electron in the laser field and ω refers to the laser frequency. $M_{nn'} = M^*_{n'n} = \langle\psi_n|\boldsymbol{\mathcal{E}}_0\boldsymbol{r}|\psi'_n\rangle$ is a dipole-coupling matrix element. $\widetilde{V}_d(\boldsymbol{\Delta},\boldsymbol{X}) = \sum_{j=1}^{Z}\exp(i\boldsymbol{\Delta}.\mathbf{r}_j) - Z$ and $G_c(\zeta) = \sum_n \frac{|\,\psi_n\rangle\langle\psi_n\,|}{\zeta - E_n}$ is the Coulomb Green's function with argument $\zeta = E_{k_i} + E_0^{\mathrm{He}} - E_q - E_{k_e} + \ell\omega$ where E_q is the virtual projectile energy.

The fully differential cross section in the SBA corresponding to the field-assisted (e, 2e) collision is given for helium atom by [30]

$$\frac{d^3\sigma^{B_2,\ell}_{ion}}{d\Omega_f d\Omega_e dE} = \frac{k_f k_e}{k_i}\left| f^\ell_{ion} - g^\ell_{ion} \right|^2, \quad (9)$$

where g^ℓ_{ion} is the exchange amplitude with the transfer of ℓ photons [28,31].

The first Born triple differential cross section accompanied by the transfer of ℓ photons is

$$\frac{d^3\sigma^{B_1,\ell}_{ion}}{d\Omega_f d\Omega_e dE} = \frac{k_f k_e}{k_i}\left| f^{B_1,\ell}_{ion} - g^\ell_{ion} \right|^2. \quad (10)$$

Note that by keeping only the first term f_1 on the right of equation (7), we obtain the first Born triple differential cross section without including target dressing effects [21].

3 Results and discussion

We are interested in demonstrating the effects of the laser frequency on the laser-assisted electron-impact ionization of helium target at low incident energies by using the second Born approximation. The fully differential cross sections are calculated in the Ehrhardt asymmetric coplanar geometry Figure 1, such that an electron of momentum $\boldsymbol{k}_i$ is incident on the atomic target, and a scattered electron of momentum $\boldsymbol{k}_f$ is detected in coincidence with an ejected electron of momentum $\boldsymbol{k}_e$, the three momenta $\boldsymbol{k}_i$, $\boldsymbol{k}_f$ and $\boldsymbol{k}_e$ being in the same plane. The angle of the scattered electron and that of the ejected electron are denoted respectively by θ_f and θ_e. θ_f is fixe and small, while θ_e is varied. We shall present our results for the following choice of scattering parameters: the incident electron energy $E_{k_i} = 40$ eV, the ejected electron energy $E_{k_e} = 5$ eV, the scattering angle $\theta_f = 4°$ and the laser field strength $\mathcal{E}_0 = 1 \times 10^7$ V/cm. The laser polarization vector $\hat{\varepsilon}$ is taken to be parallel to the incident momentum $\boldsymbol{k}_i$. In Figures 2–5, we show the variation of the triple differential cross section (TDCS) when the ionizing process is accompanied by the absorption of one photon ($\ell = 1$) for different values of the laser photon energy. We present the results of our complete computation of TDCS in the second Born approximation and compare them with those calculated in the first Born approximation and with those obtained by neglecting the target dressing effects. It is known that in a first Born treatment, two types of collision are found in the field free (e, 2e) reactions, those in which the momentum transfer to the ion produced is small (binary encounter which is attributed to the electron-electron interaction) and those in which the momentum transfer is large (recoil encounter which is governed by the attraction between the electron and the residual ion). The presence of the external laser field breaks the symmetry of the angular distribution of the ejected electron and the overall magnitude of the cross sections is significantly changed compared to the field-free case [20,21,28,29].

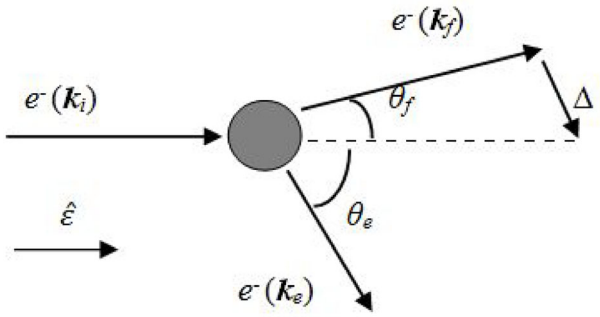

Fig. 1. Selected orientation of laser polarization for electron-impact ionization in the presence of a linearly polarized laser field.

The influence of the laser frequency is investigated by comparing Figures 2–5. In this set of figures, the polarisation orientation is taken to be parallel to the incident momentum $\boldsymbol{k}_i$ (see Fig. 1), and the electric field strength $\mathcal{E}_0$ associated to the external laser field is kept fixed. We have chosen 4 laser frequencies which are typical of laser sources currently operated, namely the near infrared ($\omega = 1.17$ eV Nd:YAG laser, Fig. 2); first harmonic of near infrared ($\omega = 2.34$ eV, Fig. 3); UV ($\omega = 6.42$ eV Ar-F laser, Fig. 4) and finally ($\omega = 8.4$ eV, Fig. 5). We have chosen to compare the TDCS computed within the first and the second Born approximations and with the results obtained by the simplified approach in which one neglects the dressing of the atomic target by the laser field. The modifications of the cross sections then directly reflect the role of the dressing of the atomic target states by the external laser

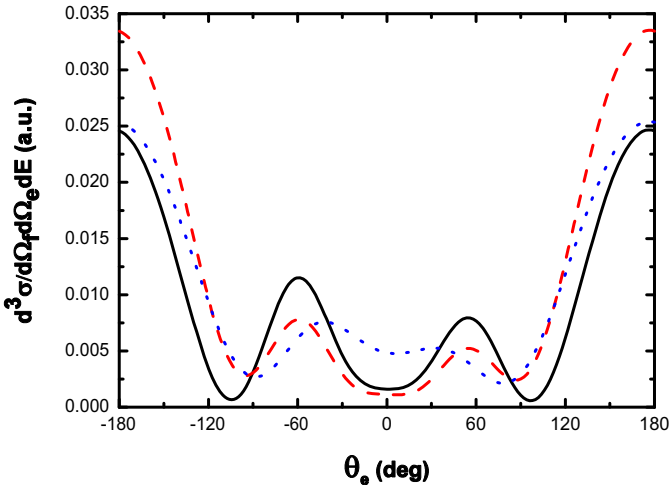

Fig. 2. Triple differential cross sections corresponding to the laser-assisted electron-impact ionization of helium atom as a function of the ejected electron angle θ_e for the absorption of one photon $\ell = 1$. The laser frequency is $\omega = 1.17$ eV and the electric field strength is $\mathcal{E}_0 = 10^7$ V/cm. The incident electron energy is $E_{k_i} = 40$ eV, the ejected electron energy is $E_{k_e} = 5$ eV, and the scattering angle is $\theta_f = 4°$. The laser polarization vector is taken to be parallel to the incident momentum $\boldsymbol{k}_i$. Solid lines: second Born approximation results. Dashed lines: first Born approximation results. Dotted lines: results obtained by neglecting the dressing of the target by the laser field.

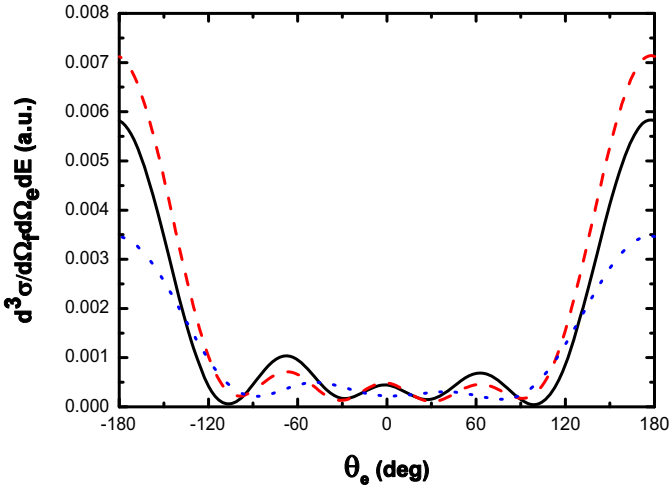

Fig. 3. All the parameters are the same as Figure 2, but for a laser frequency of $\omega = 2.34$ eV.

field. The angular distribution is strongly modified as the binary and recoil peaks are now split into smaller lobes with different magnitudes. The most remarkable feature of the cross sections dependence on the laser frequency is the fact that the dressing of the atomic target state by the external field decreases with the laser frequency. Indeed, the laser-assisted cross section varies as an inverse power of the frequency (here $\omega < 1$ a.u.), a feature which is reminiscent of the infrared divergence of quantum electrodynamics which accounts for the divergence of the bremsstrahlung and free-free cross sections in the

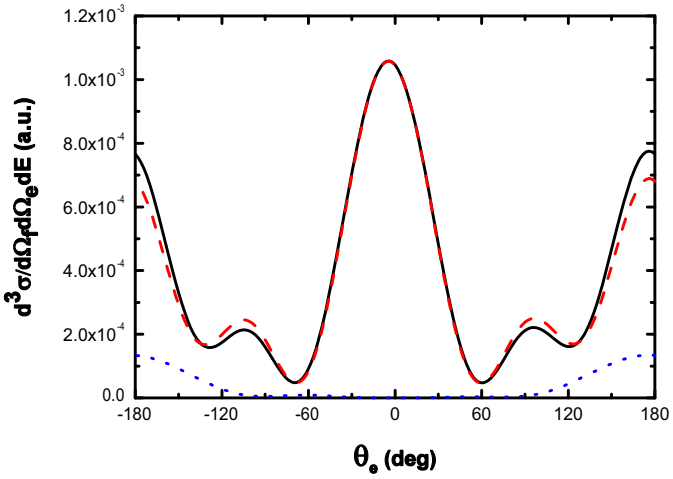

Fig. 4. All the parameters are the same as Figure 2, but for a laser frequency of $\omega = 6.42$ eV.

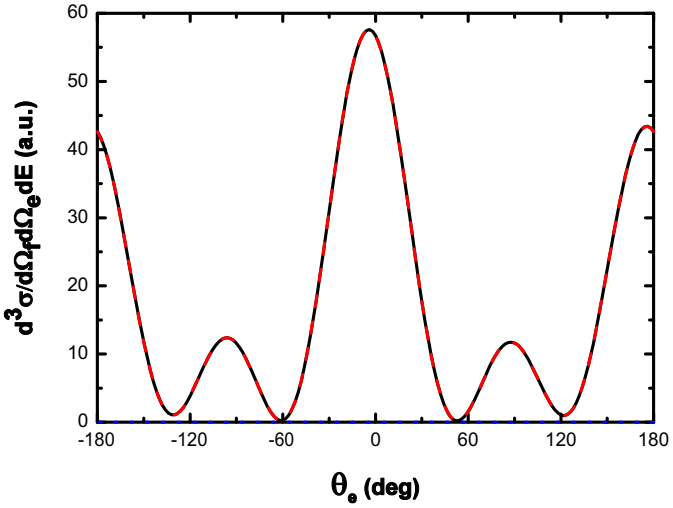

Fig. 5. All the parameters are the same as Figure 2, but for a laser frequency of $\omega = 8.4$ eV. All curves are indistinguishable.

soft-photon limit ($\omega_L \to 0$). The approximate treatment neglecting the dressing of the target regains its validity in the soft-photon regime ($\omega_L = 0.117$ eV not presented here), a result which implies that the contribution of the amplitude f_1 (Eq. (8a)) is by far dominant. This remains true when the dominance of nonperturbative effects stems from relatively large values of the arguments of the Bessel functions entering in the expressions of the transition amplitudes. The magnitude of these arguments is linked to the laser-electron coupling, the strength of which depends on the parameter $\boldsymbol{\alpha}_0 = \boldsymbol{\mathcal{E}}_0/\omega^2$. At high laser frequencies (see Figs. 4 and 5), the dressing of the atomic target by the laser field can significantly affect the TDCSs corresponding to ionizing process with the net exchange of one photon ($\ell = 1$), a result which implies that the contribution of the amplitudes f_2 and f_3 is dominant. This demonstrates that high frequency lasers, at the rather low intensities considered here, can more effectively dress bound atomic states than continuum states and we approximate

the wave function of a continuum electron by a plane wave. The other interesting point regarding the comparison between FBA and SBA results is that the margins between SBA and FBA results are large at low frequencies. When the laser photon energy increases, the gap between the two numerical results decreases (becomes almost zero). This means that the second-order correction is insignificant at high frequencies, a result which implies that the first Born approximation is sufficient in this case. In addition, one observes that the binary peaks in the SBA are enhanced and the recoil peaks are depressed with respect to the FBA at low laser frequencies. This clearly shows that the collision dynamics is strongly affected by the laser frequency, even at moderate laser intensities.

We also notice that, everything else being kept fixed, the frequency dependance effects affect more strongly the binary peak (i.e., the electron-electron interaction), while the shape of the recoil peak remains almost unchanged. This reflects the fact that the vectors $\boldsymbol{\Delta}$ and $\boldsymbol{k}_e$ are oriented in directions close to the recoil peak region (for positive values of θ_e) and in very different directions to the binary peak area (for negative values of θ_e). Therefore the parameter $\lambda = \boldsymbol{\alpha}_0 (\boldsymbol{\Delta} - \boldsymbol{k}_e)$ which characterizes the coupling of the electron-atom system with the laser field is significantly larger in the binary peak region than in the recoil peak. Note that in the absence of the laser field, the ejected momentum $\boldsymbol{k}_e$ is parallel (antiparallel) to the momentum transfer $\boldsymbol{\Delta}$ in the binary (recoil) region which constitutes a very well established fact. On the contrary, the situation seems to be reversed by the presence of the laser. The effects of the laser frequency are more manifested when the values of the ejected electron angle vary in the range $-60^\circ < \theta_e < 60^\circ$, and cause the relative decrease of the cross sections in this region when the laser frequency decreases. The behavior of binary and recoil peaks can be interpreted by the fact that the argument of the Bessel function is maximum when $\boldsymbol{k}_e$ is parallel to the momentum transfer (that is in the region of the recoil peak). Contrariwise, the argument of the Bessel function is minimum close to the binary peak, which leads to the mentioned modifications. The most remarkable feature of the dependence of the angular distribution on the laser frequency is the fact that the overall magnitude of the TDCS increases until a critical laser photon energy $\omega_c \simeq 5.432$ eV, for which the overall magnitude of the binary and recoil peaks are comparable. At this laser frequency, the cross section has the lowest value and its order of magnitude grows on both sides and the two types of collisions (binary and recoil collisions) are distributed equally at ω_c which corresponds to $E_{k_f} + E_{k_e} = E_{2^1P} - E_{1^1S}$, i.e., the laser field couples the initial state 1^1S with the first excited state of different parity before ejecting the atomic electron to the continuum. Therefore, it is convenient to distinguish between two regimes according to whether ω is smaller or larger than the critical laser photon energy ω_c.

For $\omega < \omega_c$, every other laser parameters being fixed, the electron-nucleus interaction is more important than the electron-electron attraction. One observes that the values obtained from the no-dressing treatment reproduces the shape of the angular distribution although the magnitude of the cross section is underestimated. The explicit introduction of the atomic states in dressing the initial and final state wave functions of equation (8) affects the difference in magnitude of the angular distribution, whereas for $\omega > \omega_c$, the binary peak (electron-electron interaction) becomes dominant and increases with the laser frequency compared to the recoil peak (electron-nucleus interaction). We also observe that the higher-order of the Born series becomes less important when the laser photon energy increases. In another way, for $\omega > \omega_c$ (see Figs. 4 and 5), the shape of the angular distribution in the SBA is the same as in the FBA, i.e. the second-order in the electron-atom interaction is negligible compared to the first-order. Thus, at high laser frequencies it is convenient to restrict the calculation of the TDCS corresponding to the laser-assisted electron-impact ionization of helium target to the first-order Born term. Note that in this limit, the interaction of the laser field with the incident electron is represented by a plane wave while the calculation of the first and second Born amplitudes corresponding the (e, 2e) scattering with the transfer of ℓ photons amounts to computing the contributions of the amplitudes f_2 and f_3. When considering $\omega > E_{k_e}$, the possibility arises of inducing real atomic transition via the intermediate excited states. Indeed, by suitably choosing the laser frequency and (or) the kinetic energy of the slow electron, it is possible to make the process resonant by allowing the field to couple either the initial or final states to an intermediate excited state. Such a possibility results from the resonance structure of the second-order atomic matrix elements contained in the amplitudes f_2 and f_3. The corresponding critical values of the photon energy and of the ejected electron energy are obtained from the location of the poles of these amplitudes. Explicitly, the process is resonant when

$$\omega = E_j - E_0^{\mathrm{He}} = -\frac{1}{2n^2} + 0.9037 \text{ a.u.} \tag{11}$$

and/or

$$E_{k_e} = E_j - E_0^{\mathrm{He}^+} + \omega = -\frac{1}{2n^2} + \omega \tag{12}$$

where the energies E_j are given by $E_j = E_0^{\mathrm{He}^+} + E_n^{Z=1}$ [28] where $E_n^{Z=1}$ are the hydrogen atom energies and $E_0^{\mathrm{He}} - E_0^{\mathrm{He}^+} = -0.9037$ a.u. corresponds to the first ionization energy of helium.

We notice that the contribution of the corresponding intermediate state entirely dominates the scattering amplitude when the one of the resonance conditions (11) or (12) is fulfilled. Although our model is not valid at resonance, it provides useful information concerning the qualitative behavior of the TDCSs in the vicinity of and between resonances.

Figure 6 shows TDCSs versus the laser frequency. The kinetic energies of the projectile and the ejected electron are, respectively, $E_{k_i} = 40$ eV, and $E_{k_e} = 5$ eV, while the angles of the scattered and ejected electrons are $\theta_f = 4^\circ$ and $\theta_e = 30^\circ$. The laser polarization vector is set parallel to the momentum of the incident electron. The electric field strength associated to the external laser field

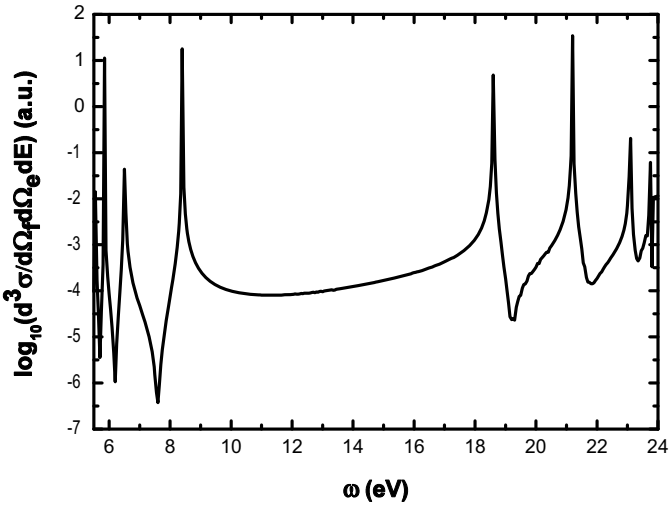

Fig. 6. Second Born Triple differential cross sections corresponding to the laser-assisted electron-impact ionization of helium atom as a function of laser photon energy ω for the absorbtion of one photon $\ell = 1$. The electric field strength is $\mathcal{E}_0 = 10^7$ V/cm, the incident electron energy is $E_{k_i} = 40$ eV, and the ejected electron energy is $E_{k_e} = 5$ eV. The scattering angle is $\theta_f = 4^\circ$ and the ejection angle is $\theta_e = 30^\circ$. The laser polarization vector is taken to be parallel to the incident momentum $\boldsymbol{k}_i$.

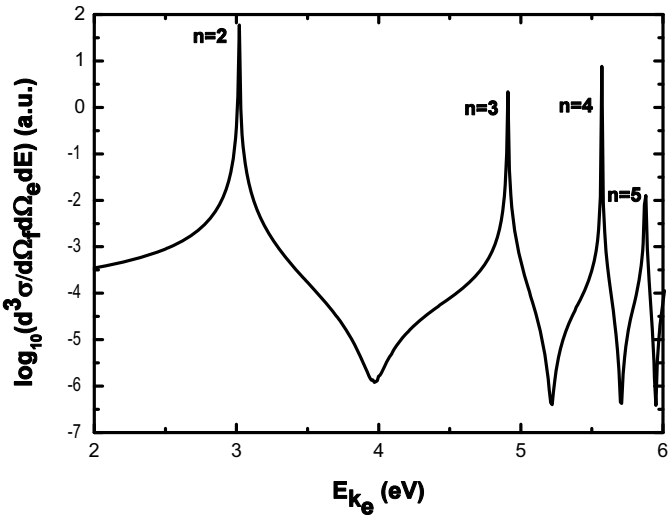

Fig. 7. Second Born Triple differential cross sections corresponding to the laser-assisted electron-impact ionization of helium atom as a function of the ejected electron energy E_{k_e} for the absorbtion of one photon $\ell = 1$. The electric field strength is $\mathcal{E}_0 = 10^7$ V/cm, the incident electron energy is $E_{k_i} = 40$ eV, and the laser photon energy is $\omega = 6.42$ eV. The scattering angle is $\theta_f = 4^\circ$ and the ejection angle is $\theta_e = 30^\circ$. The laser polarization vector is taken to be parallel to the incident momentum $\boldsymbol{k}_i$.

is $\mathcal{E}_0 = 10^7$ V/cm. This resonant structure of the cross section can be conveniently displayed by simply changing the genuinely discrete states of helium, for which one of the two electrons remains in the ground state while the other, optically active electron, has the quantum number n (principal quantum number) and l (angular quantum number) and is responsible of the sharp maxima. In Figure 6, showing abrupt changes in the vicinity of Bohr frequencies, indicate that the behavior of the cross section with respect to the laser frequency strongly depends on the structure of the He^+ target. It is also interesting to note that the results are sensitive to the presence of those Bohr frequencies, corresponding to the genuinely discrete states, even far away from resonance. This resonance occurs via the condition (11), though only np state (excited He^+ state).

Figure 7 shows the variations of the TDCS against the detection energy of the ejected electron at a fixed laser frequency $\omega = 6.42$ eV corresponding to Ar-F laser, and for a fixed angles $\theta_f = 4^\circ$ and $\theta_e = 30^\circ$. The laser polarization vector is kept parallel to the incident momentum $\boldsymbol{k}_i$. As shown in Figure 7, the cross sections can vary by several orders of magnitude, the corresponding dispersion curves in terms of E_{k_e} being characterized by the occurrence of sharp maxima separated by deep minima. The positions of the maxima are given by the resonance conditions equation (12). The observed resonant structure of the cross sections can be related to the different angular momentum distributions in the final continuum state where the coupling between the ground state to (1s 2s), (1s 2p) and (1s 2d) continues exclusively via the dipole interaction. When both resonance conditions equations (11) and (12) are fulfilled, the two amplitudes f_2 and f_3 are simultaneously resonant. This requires a purely nonperturbative treatment of the interaction between the laser field and the electron-atom system.

4 Conclusion

We have studied, in the second Born approximation, the laser-assisted differential cross sections for laser-assisted electron-impact ionization in helium. Particular attention has been paid to the laser frequency dependance of the cross sections. The importance of the dressing effects and the influence of the laser photon energy on the structure of the angular distribution of the ejected electron has been discussed in the vicinity of resonances. With laser photon energy increasing the electron-electron interaction is strongly enhanced and the shape of the recoil peak remains unchanged. Comparing with the standard first-order Born calculations, the inclusion of the second-order Born term in the ionizing amplitudes does not lead to any change in TDCSs at higher frequencies, while the laser-atom interaction is seen to be important.

References

1. B. Wallbank, J.K. Holmes, J. Phys. B **27**, 1221 (1994)
2. S. Luan, R. Hippler, H.O. Lutz, J. Phys. B **24**, 3241 (1991)
3. B. Wallbank, J.K. Holmes, Can. J. Phys. **79**, 1237 (2001)
4. F.W. Byron Jr., P. Francken, C.J. Joachain, J. Phys. B **20**, 5487 (1987)

5. P. Francken, Y. Attaourti, C.J. Joachain, Phys. Rev. A **38**, 1785 (1988)
6. M.H. Mittleman, *Introduction to the Theory of Laser Atom Interactions* (Plenum, New York, 1993)
7. P. Francken, C.J. Joachain, J. Opt. Soc. Am. B **7**, 554 (1990)
8. F. Ehlotzky, A. Jaroń, J.Z. Kamiński, Phys. Rep. **297**, 63 (1998)
9. A. Weingartshofer, J.K. Holmes, G. Gaudle, E.M. Clarke, H. Kruger, Phys. Rev. Lett. **39**, 269 (1977)
10. N.J. Mason, W.R. Newell, J. Phys B **20**, L323 (1987)
11. B. Walbank, J.K. Holmes, J. Phys. B **27**, 1221 (1994)
12. B. Wallbank, J.K. Holmes, Can. J. Phys. **79**, 1237 (2001)
13. C. Höhr, A. Dorn, B. Najjari, D. Fischer, C.D. Schröter, J. Ullrich, Phys. Rev. Lett. **94**, 153201 (2005)
14. L. Rosenberg, Adv. At. Mol. Phys. **18**, 1 (1982)
15. M. Kroll, K.M. Watson, Phys. Rev. A **8**, 804 (1973)
16. F.V. Bunkin, M.V. Fedorov, Zh. Eksp. Teor. Fiz. **49**, 1215 (1965)
17. C.J. Joachain, P. Francken, A. Maquet, P. Martin, V. Véniard, Phys. Rev. Lett. **61**, 165 (1988)
18. S. Jones, D.H. Madison, Phys. Rev. A **66**, 062711 (2002)
19. P. Martin, V. Véniard, A. Maquet, P. Francken, C.J. Joachain, Phys. Rev. A **39**, 6178 (1989)
20. D. Khalil, A. Maquet, R. Taïeb, C.J. Joachain, A. Makhoute, Phys. Rev. A **56**, 4918 (1997)
21. A. Makhoute, D. Khalil, A. Maquet, C.J. Joachain, R. Taïeb, J. Phys. B **32**, 3255 (1999)
22. R. Taïeb, V. Véniard, A. Maquet, S. Vucic, R.M. Potvliege, J. Phys. B **24**, 3229 (1991)
23. S.M. Li, J. Berakdar, S.T. Zhang, J. Chen, Phys. B **38**, 1291 (2005)
24. S.M. Li, J. Berakdar, S.T. Zhang, J. Chen, Electron Spectrosc. Relat. Phenom. **161**, 188 (2007)
25. F.H.M. Faisal, *Theory of Multiphoton Processes* (New York, Plenum, 1987)
26. D.V. Volkov, Z. Phys. **94**, 250 (1935)
27. F.W. Jr. Byron, P. Francken, C.J. Joachain, J. Phys. B **20**, 5487 (1987)
28. I. Ajana, A. Makhoute, D. Khalil, S. Chaddou, Phys. Rev. A **91**, 043411 (2015)
29. A. Makhoute, I. Ajana, D. Khalil, S. Chaddou, Eur. Phys. J. D **69**, 160 (2015)
30. C.J. Joachain, N.J. Kylstra, R.M. Potvliege, *Atoms in Intense Laser Fields* (Cambridge University Press, 2012)
31. V.I. Ochkur, Sov. Phys. J. Exp. Theor. Phys. **18**, 503 (1964)